Anisotropic tomography with rock physics constraints

Yunyue Li, Dave Nichols, Konstantin Osypov, and Ran Bachrach

ABSTRACT

Anisotropic model building is a challenging problem, well-known for its nonlinear and underdetermined nature. To reduce the null-space and stabilize the inversion, we propose a new preconditioning scheme in linearized tomography to include rock physics prior information. We introduce the rock physics information in the form of covariance among P-wave vertical velocity (v_0), ϵ and δ, and is generated by stochastic realizations of a compacting shale model. We design a VSP synthetic survey with the common industry geometry on two different examples, of which one fulfills the assumption of our rock physics model and the other does not. The results show that by utilizing the proper rock physics prior information, tomography can better resolve the anisotropy parameters, especially in the area where inversion is poorly constrained by the data. However, precautions should be taken when the lithology of the subsurface is largely unknown. Finally, we perform a posterior uncertainty analysis to evaluate the contribution of the rock physics prior information. The results show that the null-space is greatly reduced by introducing the prior information.

INTRODUCTION

Anisotropic model building tries to resolve more than one parameter at each grid point of the subsurface. This number could be 3 for a vertical transverse isotropic (VTI) media, and increase to 5 for a tilted transverse isotropic (TTI) media. Traditional surface seismic tomography may be able to produce accurate isotropic earth models efficiently for a large area when the acquisition is dense and the earth is well-illuminated by rays at a wide range of angles. However surface seismic data inversion becomes ill-posed and highly underdetermined due to the rapidly increasing dimensionalities of the model space with the increasing complexity of the subsurface.

One big disadvantage of the surface seismic tomography is the lack of the depth information. During tomography, not only is the low wavenumber earth model estimated, but the depth of the reflectors is unknown as well. To add the depth dimension into the inversion, several localized tomography experiments around the wells are analyzed (Bakulin et al., 2010d,c). In these studies, joint inversion of surface seismic data and borehole data (check-shots, walkaway VSPs) shows great potential to yield better defined earth models. However, due to the ambiguity among the parameters,

even the borehole aided localized tomography has difficulty in resolving a reliable, unique anisotropic model in 3D (Bakulin et al., 2009).

To constrain the inversion further, we need to consider some prior knowledge of the subsurface. This prior knowledge can be characterized by the covariance of the model space and is independent of the data. There are many ways to obtain the covariance information based on different assumptions. For example, we often smooth our earth model horizontally and vertically, which implies a certain user-defined spatial correlation lag. More realistically, we can use the geological information as a prior and shape our estimate accordingly. This model shaping can be posed as a decomposition of the earth model into different layers and horizons before tomography (Bakulin et al., 2010a), or as a regularization/preconditioning operator during tomography (Bakulin et al., 2010b). We can obtain the geological information either by interpreting and picking the horizons or by building a set of steering filters (Clapp, 2000) according to the current subsurface image.

In addition to the spatial covariance, for a multi-parameter estimation, a point-by-point cross-parameter covariance is also needed to fully describe the subsurface. One source of the cross-parameter covariance comes from rock physics study (Hornby et al., 1995; Sayers, 2004, 2010; Bachrach, 2010b). In particular, Bachrach (2010a) develops both deterministic and stochastic modeling schemes based on the rock physics effective media models for compacting shale and sandy shale. Along with appropriate laboratory core measurements, the parameters needed by the rock physics model are limited in a certain range, which greatly reduces the correlation lag in the earth model parameters. These rock physics modeling results can be used to construct the initial earth model and the covariance relationships among the earth model parameters. When all of these four ingredients - surface seismic, borehole traveltime measurements, geological information and rock physics priors - are available, we will have a better chance to resolve anisotropic models that both flatten the gathers and follow the geological and rock physics principles at the same time.

In this paper, we assume the spatial covariance and the local cross-parameter covariance can be fully separated and focus on utilizing the rock physics modeling results to constrain the anisotropic tomography. A VSP survey with a common industry geometry is simulated on two different models, one with only shale (sandy shale), and the other with one layer of pure sand (isotropic). We compare the inversion results using the unconstrained tomography, current constrained tomography and the rock physics constrained tomography. Finally, we perform a-posteriori uncertainty analysis (Osypov et al., 2008) for the shale example to evaluate the contribution of rock physics prior knowledge to the reduction of the null-space.

THEORY

Here, we define a VTI tomography in using event traveltime as data. To the first order, when we assume the ray path does not change with perturbation in the background

velocity model, the traveltime misfit is related to the velocity perturbation as follows:

$$\Delta t = \int_{\text{raypath}} \frac{1}{v^2} \Delta v \, \mathrm{d}\, l. \tag{1}$$

For weak anisotropy, the angle dependent velocity in VTI media can be described by vertical velocity v_0 and the Thomson anisotropic parameters ϵ and δ as follows (Tsvankin and Thomsen, 1994):

$$v(\theta) = v_0(1 + 2\delta \sin^2\theta \cos^2\theta + 2\epsilon \sin^4\theta), \tag{2}$$

where θ is the angle between propagation direction and the vertical direction. The angles are defined by the raypath in equation 1. Consequently, the velocity perturbation can be expressed as follows:

$$\Delta v(\theta) = \frac{\partial v(\theta)}{\partial v_0} \Delta v_0 + \frac{\partial v(\theta)}{\partial \epsilon} \Delta\epsilon + \frac{\partial v(\theta)}{\partial \delta} \Delta\delta. \tag{3}$$

Now we can see explicitly that the traveltime misfit has three contributions from v_0, ϵ and δ, respectively:

$$\Delta t = \int \frac{1}{v^2(\theta)} \frac{\partial v(\theta)}{\partial v_0} \Delta v_0 \, \mathrm{d}\, l + \int \frac{1}{v^2(\theta)} \frac{\partial v(\theta)}{\partial \epsilon} \Delta\epsilon \, \mathrm{d}\, l + \int \frac{1}{v^2(\theta)} \frac{\partial v(\theta)}{\partial \delta} \Delta\delta \, \mathrm{d}\, l. \tag{4}$$

In practice, we usually formulate the seismic tomography problem as an inversion problem with another model space regularization term. Then the objective function reads:

$$S(\Delta m) = ||\mathbf{T}\Delta m - \Delta t||_D^2 + ||m_0 + \Delta m - m_{\text{prior}}||_M^2, \tag{5}$$

where D denotes the data space whose covariance is $\mathbf{C_D}$ and M denotes the model space whose covariance is $\mathbf{C_M}$. In the data space fitting goal, operator $\mathbf{T}$ is a row operator vector $[\mathbf{T}_{v_0} \ \mathbf{T}_\epsilon \ \mathbf{T}_\delta]$, each element corresponding to one of the three terms in equation 4 respectively; Δm is a column model vector $[\Delta v_0 \ \Delta\epsilon \ \Delta\delta]'$; Δt is the traveltime misfit. In the model space fitting goal, m_0 is the background (initial) model $[v_{0_0}, \epsilon_0, \delta_0]'$; m_{prior} is the mean of the prior distribution in the model space $[v_{0p}, \epsilon_p, \delta_p]'$. We evaluate both fitting goals in L2 using an LSQR solver.

We can also obtain the normal equation representation of the objective function by taking the derivative of equation 5 with respect to Δm:

$$\begin{vmatrix} \mathbf{C_D^{-1/2}T} \\ \lambda \ \mathbf{C_M^{-1/2}} \end{vmatrix} \Delta m = \begin{vmatrix} \mathbf{C_D^{-1/2}} \Delta t \\ \lambda \ \mathbf{C_M^{-1/2}} (m_{\text{prior}} - m_0), \end{vmatrix} \tag{6}$$

where λ is the balancing factor between the data fitting equation and the model fitting equation. For the synthetic study here, we may assume $\mathbf{C_D} = \mathbf{I}$, since there is no noise in these data.

To speed up the convergence, we turn this regularized problem into a preconditioned problem by doing a variable substitution:

$$\begin{vmatrix} \mathbf{T}\mathbf{C}_{\mathbf{M}}^{\mathbf{1/2}} \\ \lambda\ \mathbf{I} \end{vmatrix} \Delta m' = \begin{vmatrix} \Delta t \\ \lambda\ \mathbf{C}_{\mathbf{M}}^{\mathbf{-1/2}}(m_{\text{prior}} - m_0) \end{vmatrix}. \tag{7}$$

Now LSQR inverts the preconditioning variable $\Delta m'$, and the real model updates are obtained by $\Delta m = \mathbf{C}_{\mathbf{M}}^{\mathbf{1/2}} \Delta m'$ after inversion.

For a multi-parameter model inversion, we assume the model covariance can be fully decoupled into two different parts: spatial covariance for each parameter, and the local cross-parameter covariance. Mathematically, that translates into:

$$\mathbf{C}_{\mathbf{M}}^{\mathbf{1/2}} = \mathbf{S}\sigma = \begin{vmatrix} \mathbf{S_v} & 0 & 0 \\ 0 & \mathbf{S}_\epsilon & 0 \\ 0 & 0 & \mathbf{S}_\delta \end{vmatrix} \begin{vmatrix} \sigma_{vv} & \sigma_{v\epsilon} & \sigma_{v\delta} \\ \sigma_{\epsilon v} & \sigma_{\epsilon\epsilon} & \sigma_{\epsilon\delta} \\ \sigma_{\delta v} & \sigma_{\delta\epsilon} & \sigma_{\delta\delta} \end{vmatrix}, \tag{8}$$

where $\mathbf{S}$ is a spatial smoothing matrix, and σ is the square-root of the point-by-point cross-parameter covariance matrix. Each element of $\mathbf{S}$ can be estimated according to the user's assumption for the smoothness of different parameters. For example, the steering filters (Fomel, 1994; Clapp et al., 2004) provide a good choice to incorporate the structural information of the subsurface. The local cross-parameter covariance can be estimated from the rock physics modeling (Bachrach, 2010a).

The left panel on Figure 1 shows an example of the stochastic realizations of a rock physics model for shale and sandy shale. The dots are scattered v_0, ϵ and δ results of hundreds of realizations, while the nine ellipsoids are fitted locally with v_0 the controlling variable to describe the multi-Gaussian relationship among the parameters. With a statistical study of the laboratory measurements on the cores, the range of the required input parameters for the rock physics model has been limited to a relatively narrow range, which leads to tight ellipsoids in Figure 1. We refer interested readers to details in Bachrach (2010a).

In this paper, we build the cross-parameter covariance matrix for each grid point in the subsurface according to the velocity, and linearly interpolate between the ellipsoids to which the velocity value belongs. Notice that additional non-linearity has been introduced during this process. Better methods to utilize the stochastic realizations could fit ellipsoids centered at every velocity value, which can be more precise but outside the scope of this study.

NUMERICAL TESTS

We design a walkaway VSP survey on a 2D study area shown in Figure 2. There are 51 sources distributed evenly along a 5 km line on the surface with 2.5 km maximum offset, and 10 receivers fixed every 1 km down the borehole. This acquisition geometry is designed to be similar to the industry standard VSP surveys, which have good

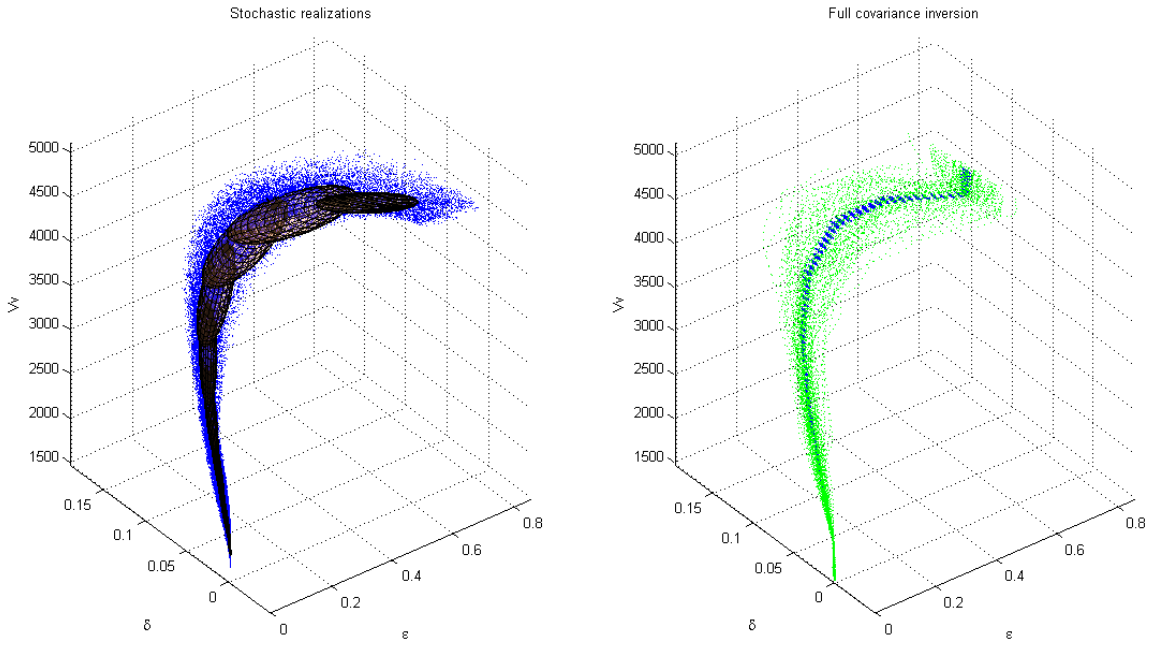

Figure 1: Left: Stochastic realizations of a rock physics modeling for shale and sandy shale. The ellipsoids are fitted locally to describe the multi-Gaussian relationship among the parameters. Right: Small dots in the background are the estimated prior distribution by the operator using the ellipsoids on the left. Larger dots are the null-space projection of the operator. [**NR**]

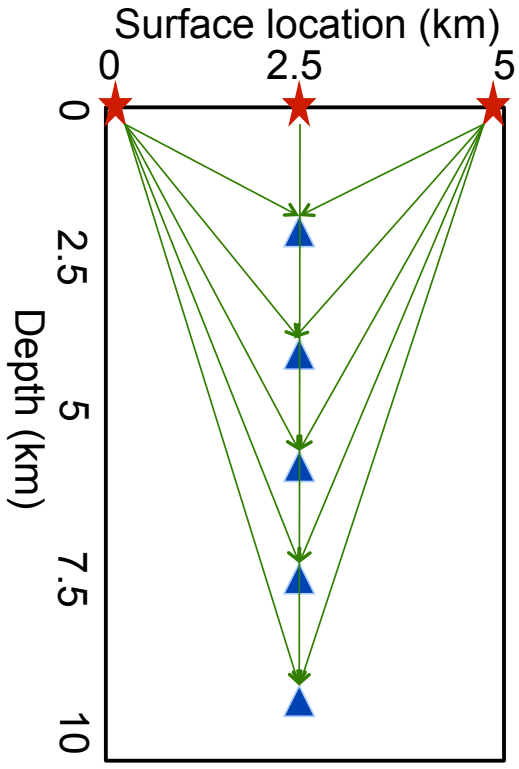

Figure 2: Walkaway VSP acquisition geometry. [**NR**]

constraints for vertical velocity and δ, but fewer constraints for ϵ in the deeper part due to the limited propagation angles.

Two 1.5D models are evaluated using this method. One is a shale (sandy shale) model which completely follows the covariance matrix we generated from the rock physics modeling; the other is the same except for a layer of isotropic sand where the prior information is "wrong".

Now we are ready to test our method using different prior information. For different tests, we apply the same smoothing operator $\mathbf{S}$, but different estimates of point-by-point cross-parameter covariance σ. In the notations below, "no prior" means $\sigma = \mathbf{I}$; "column weighting" means σ has only diagonal elements which are constant for every grid point in the subsurface; "diagonal covariance" means σ has only diagonal elements which vary according to the rock physics modeling results; "full covariance" means σ has all nine elements which vary according to the rock physics prior for each grid point in the subsurface.

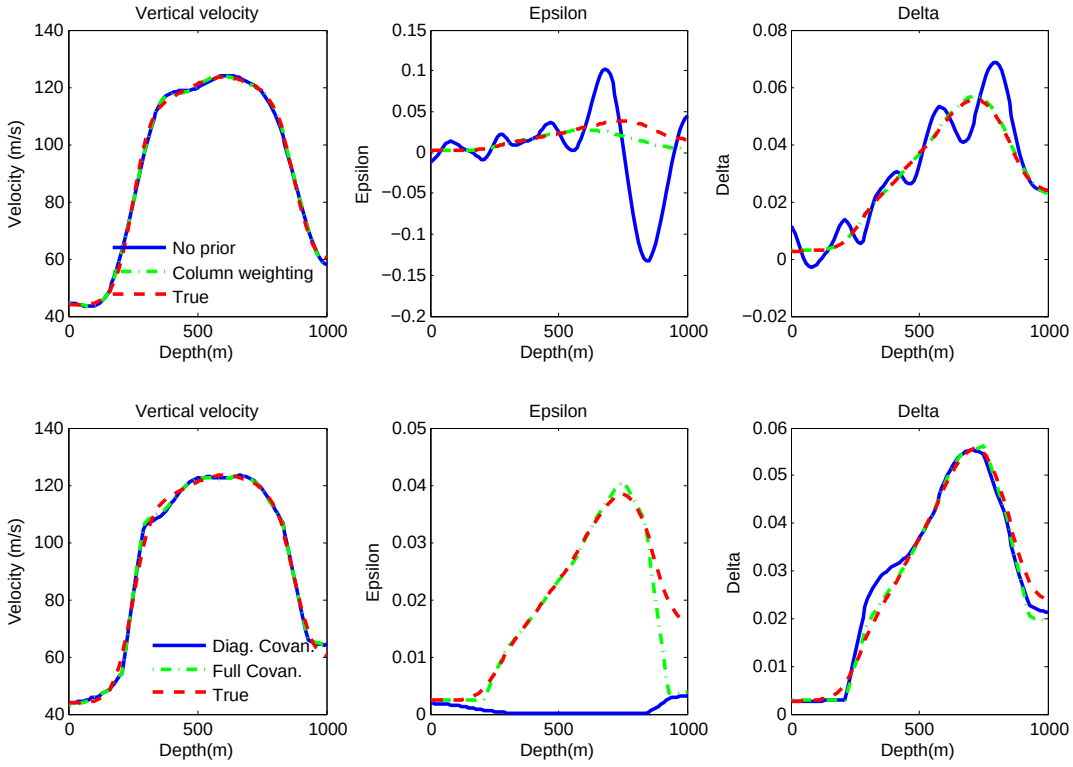

Figure 3: Inversion results of the shale (sandy shale) model. Panels on the left show the velocity perturbation, in the middle ϵ perturbation, and on the right δ perturbation. The top row shows the inversion results without rock physics prior knowledge: Solid line: No prior; Dashed dot line: Column weighting; Dashed line: True model. The bottom row shows the inversion results with some rock physics knowledge: Solid line: Diagonal covariance; Dashed dot line: Full covariance; Dashed line: True model. [**NR**]

Figure 3 shows the inversion results of the shale (sandy shale) model. It is obvious that vertical velocity is the best constrained variable, therefore, all inversion schemes yield good estimations for vertical velocity. However, instability is seen in the results of ϵ and δ when no prior information is included. The oscillations in ϵ and δ are out-of-phase, which is the numerical proof for the theoretical predicted trade-off between these two parameters. Inversion with column weighting yields more stable results for δ and the shallow part of ϵ. For the deeper part and also less constrained part of ϵ, column weighting gives a less satisfactory result. When rock physics prior knowledge is introduced, the inversion is further stabilized. Both the diagonal and the full covariance give good estimations for velocity and δ, while superior result for ϵ is obtained by full covariance since correct prior knowledge adds information to the inversion. The fact that a much closer estimation for ϵ was produced using full covariance rather than the diagonal one suggests that large cross-terms exist in the covariance matrix.

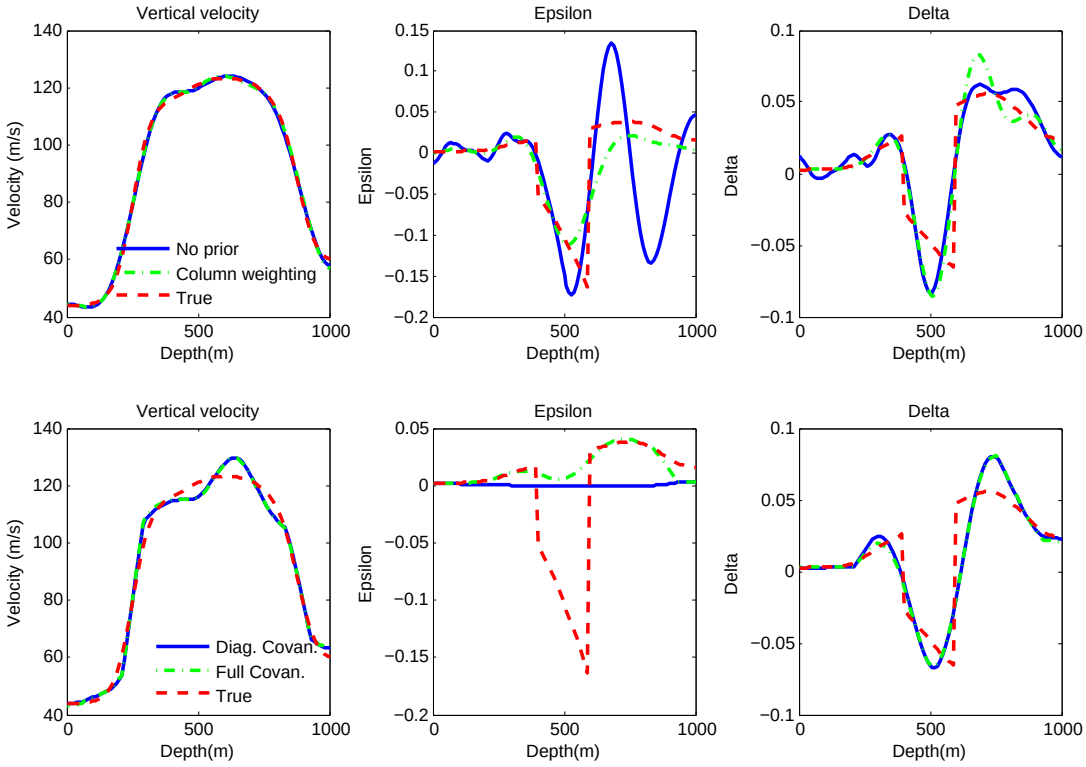

Figure 4: Inversion results of the shale model with an isotropic sand layer. Panels are arranged in the same order as Figure 3. [**NR**]

Figure 4 shows the inversion results of the shale (sandy shale) model with an isotropic layer in the middle. Similar stability conclusions can be drawn as for the shale (sandy shale) case. Notice that for the well-constrained variable δ, inversion is able to resolve the isotropic layer even though "wrong" prior information is provided. However, the inversion result is highly biased towards the prior information for ϵ where it is not so well constrained.

POSTERIOR UNCERTAINTY ANALYSIS

For a regularized problem, an L-curve analysis is often useful to determine the damping parameter λ in equation 7 and investigate the posterior distribution of the inversion (Hansen and O'Leary, 1993). Typical L-curve has two distinct parts: one vertical part where the solution is dominated by the data fitting and one horizontal part where the solution is dominated by the model styling. The corner of the L-curve corresponds to a good balance between minimization of both fitting goals. In Figure 5, we obtain the L-curve for each inversion scheme for the shale (sandy shale) model in log-log scale by varying λ from $1e-11$ to 0.1. The model residual is defined in the preconditioning space. Therefore, the shape of the L-curve also depends on the covariance matrix. A good estimation of the covariance and a proper λ will place the solution right at the corner of the L-curve, as in the case of using the full covariance. The "7-curve" shape in the log-log scale (which is still an "L-curve" in absolute scale) shows a relatively poor estimation of the covariance matrix, hence indicating difficulties in finding a proper damping parameter λ.

Finally, to move beyond the deterministic inversion which produces only one solution, we perform the null-space analysis following the work flow proposed by Osypov et al. (2008). The effective null-space of an operator can be sampled by an iterative Lanczos eigen-decomposition method. The right panel on Figure 1 shows the null-space projection (darker dots) overlaid on the approximate prior distribution (smaller dots) when the full covariance scheme is used. It is obvious that the full covariance matrix representation produces a good estimation to the true prior (by the similarity of the cloud shape on the left panel and the right panel). Also, the null-space projection suggests that higher uncertainty in anisotropic parameters for higher velocities, which often means greater depth, is embedded in rock physics knowledge. The reduced volume of the cloud shows the value of information that the data bring into the inversion.

CONCLUSIONS

In this paper, we have proposed a new formulation to incorporate rock physics prior information with the anisotropic tomography. Two models were analyzed using this method, and the inversion results demonstrate the trade-off among the parameters and the instability due to the huge null-space when no prior information is included. Any estimation of the local cross-parameter distribution (column weighting, diagonal covariance and full covariance) is helpful to stabilize the inversion and leads to a better representation of the subsurface. However, we should be careful in using too tight of a prior distribution when the lithology is uncertain, especially for areas where parameters are not well-constrained by the data. The posterior distribution analysis shows that by adding the rock physics prior information, we will obtain a better estimation of the true prior statistics in the inversion and a smaller uncertainty in the posterior statistics.

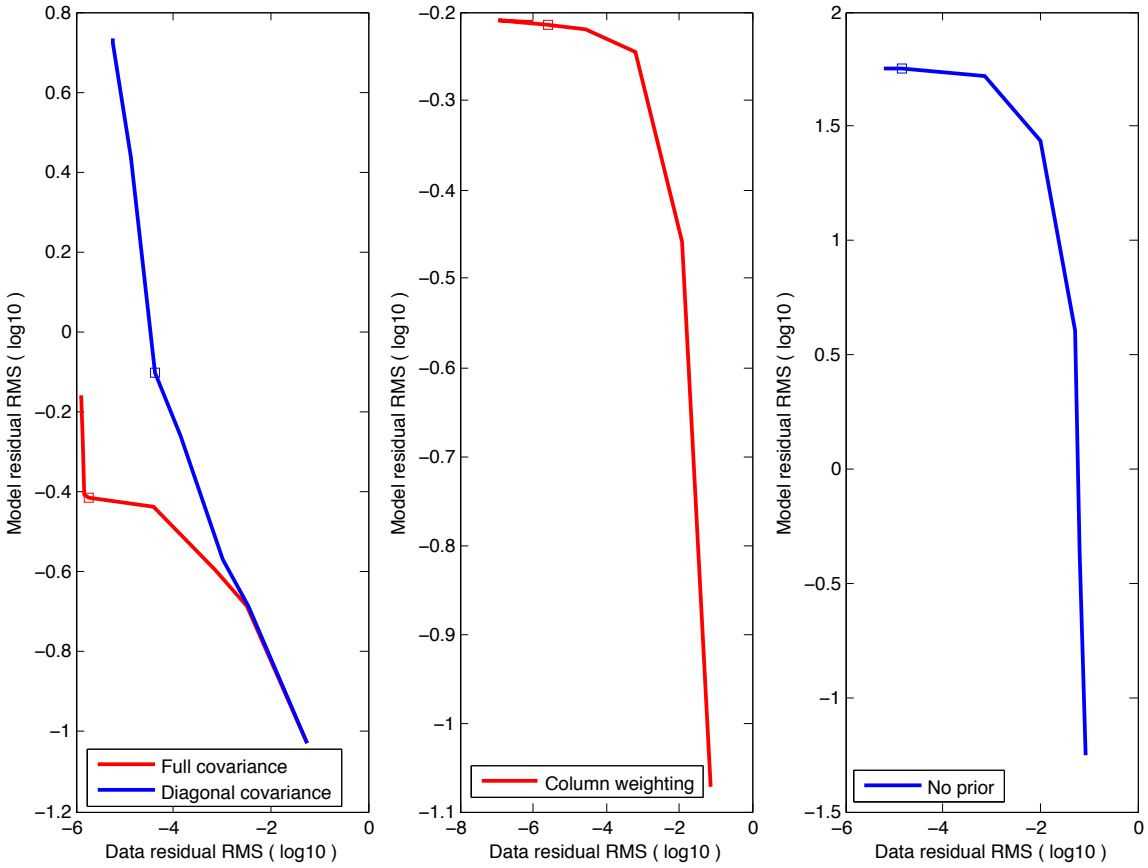

Figure 5: L-curve for the shale (sandy shale) model inversion. [**NR**]

The experiment of rock physics constrained tomography suggests to us a new workflow in anisotropic model building.

- First, Build an initial model using the deterministic rock physics modeling and obtain the initial image.
- Second, Build the point-by-point cross-parameter covariance according to the stochastic rock physics modeling. Build the spatial covariance using geology information and/or the initial image.
- Third, run the rock physics constrained joint tomography with surface seismic data and borehole data.

Repeat the workflow if necessary. Up to now, it is possible to use all the information: surface reflection seismic, borehole data, geological estimation and the rock physics covariance in the tomography to produce a unique earth model that explains the seismic data and satisfies the geological and rock physics theory at the same time.

ACKNOWLEDGEMENT

This work was completed during my summer internship with WesternGeco in 2010. The results were produced based on the C++ library in WesterGeco, and hence NR to non-WesternGeco sponsors. The authors thank WesternGeco for the permission to publish this work. Thanks to Marta Woodward, Can Evren Yarman, Yangjun Liu, Xiang Xiao, Feng Qiao for helpful discussions.

REFERENCES

Bachrach, R., 2010a, Applications of deterministic and stochastic rock physics modeling to anisotropic velocity model building: SEG Expanded Abstracts, **29**, 2436–2440.

———, 2010b, Elastic and resistivity anisotropy of compacting shale: Joint effective medium modeling and field observations: SEG Expanded Abstracts, **29**, 2580–2584.

Bakulin, A., Y. K. Liu, O. Zdraveva, and K. Lyons, 2010a, Anisotropic model building with wells and horizons: Gulf of mexico case study comparing different approaches: The Leading Edge, **29**, 1450–1460.

Bakulin, A., M. Woodward, Y. Liu, O. Zdraveva, D. Nichols, and K. Osypov, 2010b, Application of steering filters to localized anisotropic tomography with well data: SEG Expanded Abstracts, **29**.

Bakulin, A., M. Woodward, D. Nichols, K. Osypov, and O. Zdraveva, 2009, Can we distinguish TTI and VTI media?: SEG Expanded Abstracts, **28**, 226–230.

———, 2010c, Building tilted transversely isotropic depth models using localized anisotropic tomography with well information: Geophysics, **75**, 27–36.

———, 2010d, Localized anisotropic tomography with well information in VTI media: Geophysics, **75**, 37–45.

Clapp, R., 2000, Geologically constrained migration velocity analysis: PhD thesis, Stanford University.

Clapp, R., B. Biondi, and J. Claerbout, 2004, Incorporating geologic information into reflection tomography: Geophysics, **69**, 533–546.

Fomel, S., 1994, On model-space and data-space regularization: A tutorial: Stanford Exploration Project Report, **94**, 141–160.

Hansen, P. C. and D. P. O'Leary, 1993, The use of the the L-curve in the regularization of discrete ill-posed problems: SIAM J. Sci. Comput., **14**, 1487–1503.

Hornby, B., D. Miller, C. Esmersoy, and P. Christie, 1995, Ultrasonic-to-seismic measurements of shale anisotropy in a North Sea well: SEG Expanded Abstracts, **14**, 17–21.

Osypov, K., D. Nichols, M. Woodward, O. Zdraveva, and C. E. Yarman, 2008, Uncertainty and resolution analysis for anisotropy tomography using iterative eigendecomposition: SEG Expanded Abstracts, **27**, 3244–3249.

Sayers, C., 2004, Seismic anisotropy of shales: What determines the sign of Thomsen's delta parameter?: SEG Expanded Abstracts, **23**, 103–106.

———, 2010, The effect of anisotropy on the Young's moduli and Poisson's ratios of shales: SEG Expanded Abstracts, **29**, 2606–2611.

Tsvankin, I. and L. Thomsen, 1994, Nonhyperbolic reflection moveout in anisotropic media: Geophysics, **59**, 1290–1304.